Electronic Supplementary Material (ESI) for Catalysis Science & Technology.

Nickel Selenide as Efficient Electrocatalyst for Selective Reduction of Carbon Dioxide to Carbon-rich Products

Apurv Saxena[a], Wipula P. R. Liyanage[a], Shubhender Kapila[a], Manashi Nath[a]*

Supporting Information

Identification and quantification of liquid products

NMR spectroscopy

Liquid products formed during CO_2 electrochemical reduction were analyzed with ^{1}H-NMR. Aliquots were collected at regular intervals as mentioned in the manuscript and 2 µL DMSO (internal standard) and 200 µL D_2O was added to 0.5 ml electrolyte. The NMR experiments were performed on a Bruker 400 MHz NMR spectrometer, using a presaturation sequence to suppress the water signal. NMR spectra of reaction mixture was measured before starting any electrochemical reaction to make sure that there was no impurity in the solution which can lead to false results.

Table S1. Chemical shifts and assignments of peaks from different possible products observed in 1H-NMR spectra after CO_2 reduction.

Observed NMR Values			Products		Standard NMR Values[47]
Chemical Shift	1H Splitting	J coupling	Probed Nucleus	Name	Chemical Shift
8.35	s		$CHOO^-$	Formate	8.35
3.64	q	7.08	$CH3CH_2OH$	Ethanol	3.64
3.23	s		CH_3OH	Methanol	3.23
1.8	s		$CH_3C(=O)O^-$	Acetate	1.8
1.20	t	7.16	CH_3CH_2OH	Ethanol	1.20

Quantification of the products

Liquid products were quantified from NMR spectra by calibrating it with respect to the internal standard and quantifying the identified products.

Gaseous products of CO_2 reduction were collected and transferred to GC using gas-tight syringe. The GC was equipped with thermal conductivity detector (GC- TCD) and Molecular Sieve 5A capillary column. Helium (99.999%) was used as the carrier gas. The GC columns led directly to a TCD detector to quantify hydrogen and carbon monoxide. At ambient conditions, CO_2 was continuously purged through a cathode compartment flow cell at a rate of 20 sccm while a constant potential was applied for designated time. The cell effluent was sampled using 100 µL syringe.

The Faradaic efficiency (FEs) was calculated by measuring the current and using mole percentages quantified through GC-TCD as well as NMR analysis as follows:

Table S1: Calculated Faradaic Efficiency along with product concentration obtained at -1.3 V vs RHE.

Products	No. of moles of product(mol)	*n* (number of electrons required to form specific product)	C_e (Charge required to form certain product) (C)	FE = C_e /C_T*100
H_2	2.83627E-06	2	0.547314379	1.266931432
formate	3.63399E-05	2	7.012509647	16.23266122
ethanol	0	12	0	0
acetate	3.43726E-05	8	26.53154813	61.41562068
Methanol	1.29243E-05	6	7.481982747	17.31940451

Table S2: Calculated Faradaic Efficiency along with product concentration obtained at -0.9 V vs RHE.

Products	No. of moles of product(mol)	*n* (number of electrons required to form specific product)	C_e (Charge required to form certain product) (C)	FE = C_e /C_T*100
H_2	1.0523E-06	2	0.203062331	0.564062031
Formate	7.47992E-06	2	1.443400686	4.009446351
Ethanol	5.46773E-06	12	6.330646802	17.58513
Acetate	2.24623E-05	8	17.33820268	48.16167412
Methanol	1.56143E-05	6	9.039280197	25.10911166

Table S3: Calculated Faradaic Efficiency along with product concentration obtained at -0.6 V vs RHE.

Products	No. of moles of product(mol)	*n* (number of electrons required to form specific product)	C_e (Charge required to form certain product) (C)	FE = C_e /C_T*100
H_2	2.41366E-07	2	0.046576365	0.215631319
Formate	0	2	0	0
Ethanol	1.34583E-05	12	15.58232909	72.14041245
Acetate	4.71388E-06	8	3.638550456	16.845141
Methanol	2.52189E-06	6	1.459946464	6.759011406

Table S4: Calculated Faradaic Efficiency along with product concentration obtained at -0.25 V vs RHE.

Products	No. of moles of product(mol)	*n* (number of electrons required to form specific product)	C_e (Charge required to form certain product) (C)	FE = C_e /C_T*100
H_2	0	2	0	0
Formate	0.00E+00	2	0	0
Ethanol	0	12	0	0
Acetate	9.18E-06	8	7.088056034	98.45
Methanol	0	6	0	0

Table S5: Calculated Faradaic Efficiency along with product concentration obtained at -0.1 V vs RHE.				
Products	No. of moles of product(mol)	*n* (number of electrons required to form specific product)	C_e (Charge required to form certain product) (C)	FE = C_e /C_T*100
H_2	0	2	0	0
Formate	0	2	0	0
Ethanol	0	12	0	0
Acetate	3.67314E-06	8	2.835222414	97.22984958
Methanol	0	6	0	0

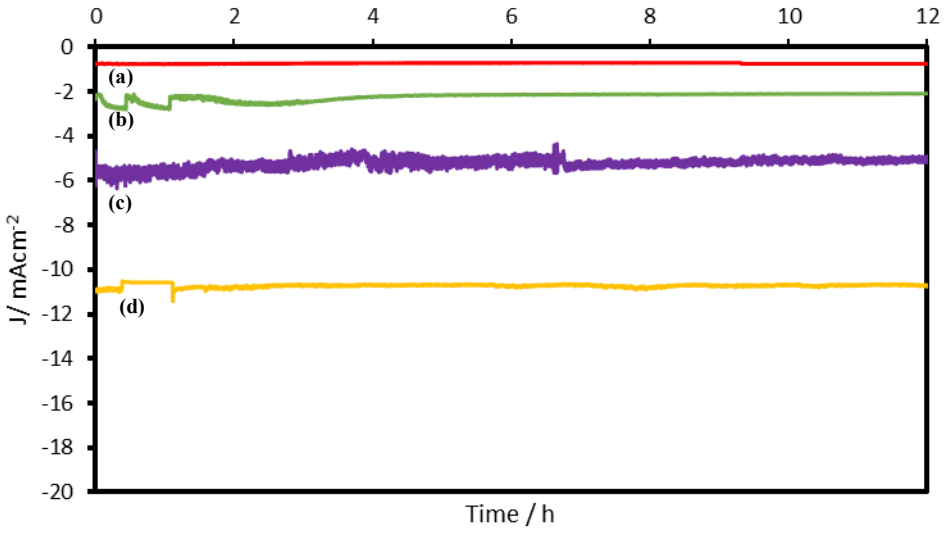

Figure S1. Current density plot for 12 h of chronoamperometry study at different applied potential: (a) -0.1V vs RHE, (b) -0.25V vs RHE, (c) -0.6V vs RHE, (d) -0.9V vs RHE

Use of widely accepted experimental procedures

We followed data collections methods and protocol as outlined in, "Standards and Protocols for Data Acquisition and Reporting for Studies of the Electrochemical Reduction of Carbon Dioxide" [1] (referred to as Standards paper, hereafter). All our measurements, data collection protocols and reporting follow the guidelines provided in the above-mentioned paper very closely. All our electrochemical experiments have been performed in magnetically stirred solution under rapid bubbling with CO_2 gas to reduce the limitations of mass transfer, as has been suggested in the Standards paper. Limitations to mass transfer can also be reduced by reducing surface roughness of the electrodes and using flat surfaces. All our electrocatalytic experiments have been performed on flat carbon fiber paper electrodes with minimal surface roughness.

As recommended in the Standards paper, we refrained from using Pt as counter electrode to minimize leaching and eventual impurity enrichment in the electrolyte and near the electrode which can lead to unexpected conversions and erroneous data. All our electrocatalytic reactions has been performed with glassy carbon as counter electrode. Additionally, we have characterized the electrodes and electrolyte with XPS, EDS, and ICP-MS which shows the presence of only Cu, and Se, and no other impurity atoms confirming purity of the system.

The Standards paper suggested benchmarking of the catalysts by comparing with systems polycrystalline Ag. We calibrated our electrochemical setup by measuring CO2RR activity with polycrystalline silver electrode. Polycrystalline silver electrode in our experimental setup shows similar performance (formation of CO, H_2, and formic acid, at -0.9 V vs RHE applied potential) as has been reported in various studies,[1–3] validating the accuracy of our electrochemical setup. The NMR analysis for products formed from polycrystalline Ag and $NiSe_2$ electrode confirms the presence of methanol, ethanol and acetic acid for $NiSe_2$ electrode. Also, the current-density plot of Ag@carbon cloth in presence of CO_2 matches with already done studies (Figure S2 below)[2,3] All our CO2RR experiments were performed in NaHCO3 electrolyte without presence of any other alkali metal ions, which may lead to erroneous data as has been indicated in the

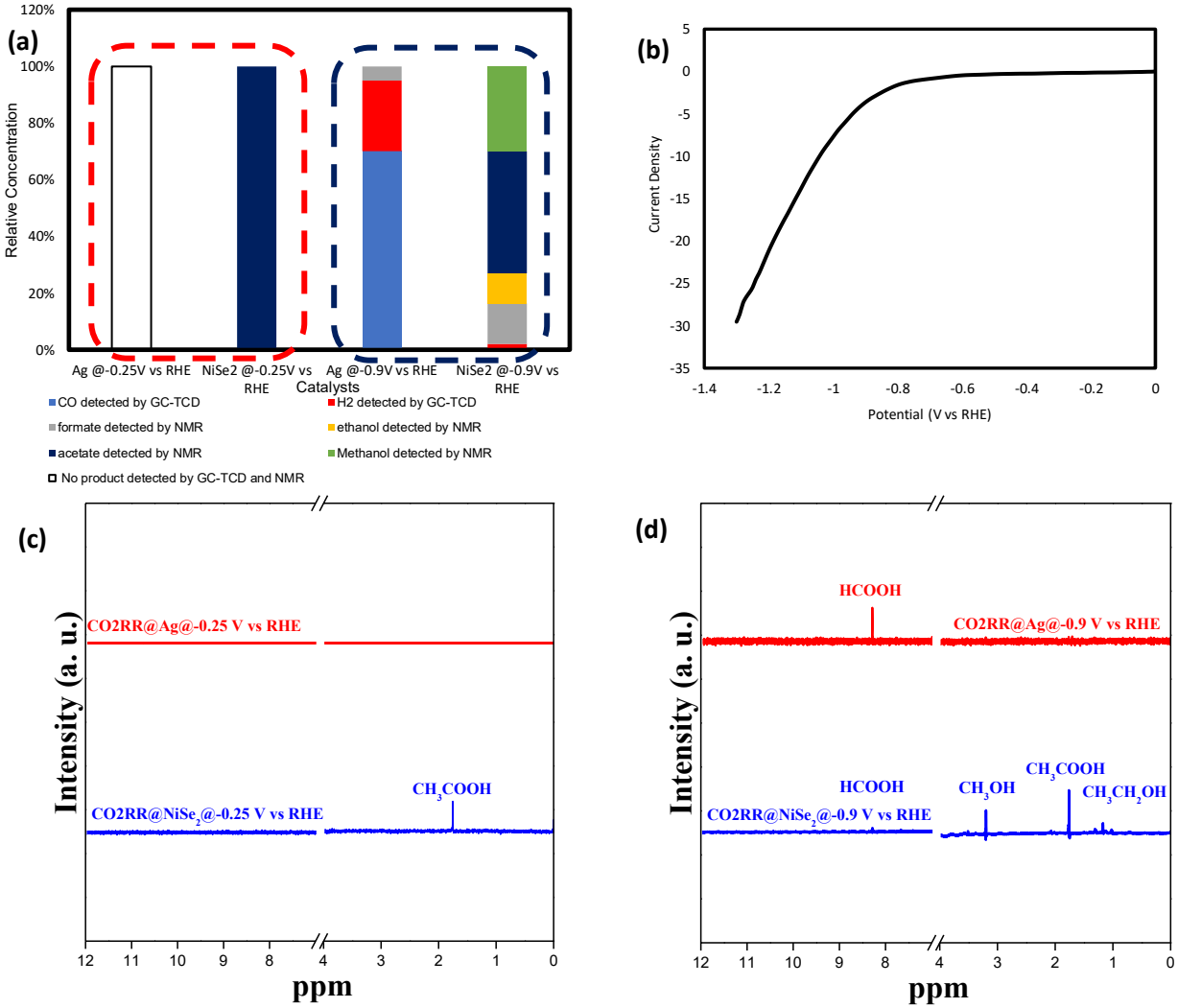

Figure S2. Comparison of CO2RR activity with (a) polycrystalline Ag film synthesized in the authors' lab with $NiSe_2$. The polycrystalline Ag tested in the authors laboratory showed formation of CO, HCOOH, and H_2 at -0.9 V vs RHE, while no product was detected with NMR and GC-TCD at -0.25 V (after 2-6 h). The $NiSe_2$ sample on the other hand, showed distinct presence of acetic acid, ethanol, methanol, and formic acid at -0.9 V, while at -0.25 V it shows exclusive formation of acetic acid. (b) LSV plots of polycrystalline Ag measured in the author's laboratory which matched with that of reported literature[refs]. (c) and (d) shows comparison of the NMR analysis of CO2RR products formed with polycrystalline Ag and $NiSe_2$ at -0.25 V and -0.9 V, respectively.

Standards paper. We have also reported ECSA and product-specific current density as has been suggested in the Standards paper.

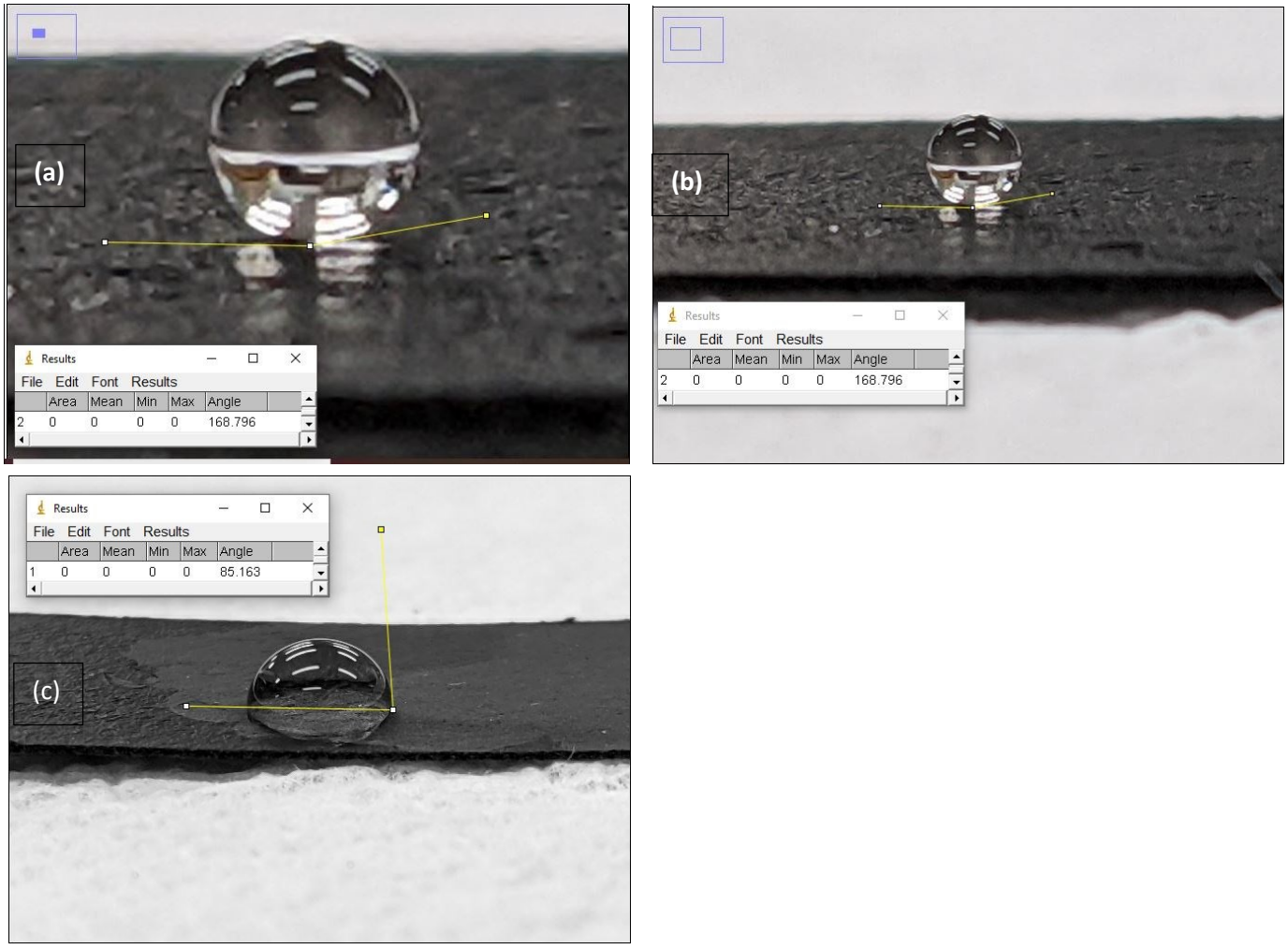

Figure S3. (a, b) Photograph of water droplets on CFP. (c) Photograph of water droplets on $NiSe_2$@CFP illustrating better wetting interaction on the $NiSe_2$-modified electrode.

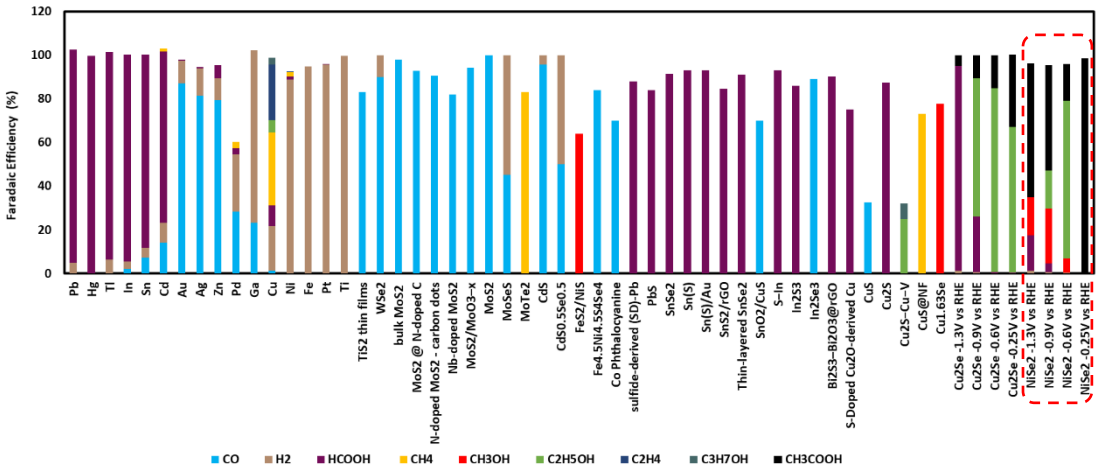

Figure S4. Comprehensive comparison of products obtained through electrocatalytic CO2RR with $NiSe_2$ and other catalysts as assembled from various reports published from different research groups

Details of DFT Calculation:

Adsorption energies of CO on the $NiSe_2$ catalyst surface was calculated by fully periodic plane-wave density functional theory (DFT) using the Vienna Ab-initio Simulation Package (VASP)[4] with the exchange-correlation functional Perdew–Burke–Ernzerhof (PBE)[5] within the generalized gradient approximation (GGA)[6] implemented with the Projector Augmented Wave function (PAW)[7] method. The relaxations of the atoms were carried out by conjugate gradient algorithm until atomic forces of the system were smaller than 0.01eV without any constrains and the search for optimal geometries were performed using a cut-off for the plane-wave basis set of 500 eV with the convergence criteria for electronic self-consistent iterations set at 1.0×10^{-6} eV. The Methfessel–Paxton smearing with a value of smearing parameter σ of 0.2 eV was applied to the orbital occupation. The Brillouin zones of all surfaces were sampled with 7×5×3 Monkhorst-Pack[8] grids. For each species, surface models with unit cells of 2x2x4 with a vacuum region of 15 Å along z-direction were used. First the free surfaces were relaxed to obtain the energy of the clean surface, E_{clean}, and then CO was placed on top of active sites of the catalyst at a distance of ~ 1.80 Å, which is very close to the equilibrium distance of CO on transition metal sites, and the system was allowed to relax to calculate, E_{sys}, the total formation energy of the system. The adsorption energy of CO, E_{ad}, was calculated as $E_{ad} = E_{sys} - E_{clean} - E_{CO}$, in which E_{CO} is the energy of free CO.

References

1 E. L. Clark, J. Resasco, A. Landers, J. Lin, L. T. Chung, A. Walton, C. Hahn, T. F. Jaramillo and A. T. Bell, Standards and Protocols for Data Acquisition and Reporting for Studies of the Electrochemical Reduction of Carbon Dioxide, *ACS Catal.*, 2018, **8**, 6560–6570.

2 W. Qiu, R. Liang, Y. Luo, G. Cui, J. Qiu and X. Sun, A Br− anion adsorbed porous Ag nanowire film: in situ electrochemical preparation and application toward efficient CO2 electroreduction to CO with high selectivity, *Inorg. Chem. Front.*, 2018, **5**, 2238–2241.

3 Y. Yu, N. Zhong, J. Fang, S. Tang, X. Ye, Z. He and S. Song, Comparative Study between Pristine Ag and Ag Foam for Electrochemical Synthesis of Syngas with Carbon Dioxide and Water, *Catal. 2019, Vol. 9, Page 57*, 2019, **9**, 57.

4. Kresse, G., & Furthmüller, J. (1996). Efficient iterative schemes for ab initio total-energy calculations using a plane-wave basis set. Physical review B, 54(16), 11169.

5. Perdew, J. P., Burke, K., & Ernzerhof, M. (1996). D. of Physics, NOL 70118 J. Quantum Theory Group Tulane University. Phys. Rev. Lett, 77, 3865-3868.

6. Perdew, J. P., Chevary, J. A., Vosko, S. H., Jackson, K. A., Pederson, M. R., Singh, D. J., & Fiolhais, C. (1992). Atoms, molecules, solids, and surfaces: Applications of the generalized gradient approximation for exchange and correlation. Physical review B, 46(11), 6671.

7. Blöchl, P. E. (1994). Projector augmented-wave method. Physical review B, 50(24), 17953.

8. Monkhorst, H. J., & Pack, J. D. (1976). Special points for Brillouin-zone integrations. Physical review B, 13(12), 5188.